Annales Societatis Geologorum Poloniae (2018), vol. 88: 341–359 doi: https://doi.org/10.14241/asgp.2018.022

NEW INSIGHTS INTO THE GLACIAL HISTORY OF SOUTHWESTERN POLAND BASED ON LARGE-SCALE GLACIOTECTONIC DEFORMATIONS – A CASE STUDY FROM THE CZAPLE II GRAVEL PIT (WESTERN SUDETES)

Aleksander KOWALSKI[1, 2], Małgorzata MAKOŚ[1] & Mateusz PITURA[1]

[1]*Department of Structural Geology and Geological Mapping, Institute of Geological Sciences, University of Wrocław, pl. M. Borna 9, 50-204 Wrocław, Poland;*
e-mails: aleksander.kowalski@uwr.edu.pl, malgorzata.makos2@uwr.edu.pl mateusz.pitura2@uwr.edu.pl
[2]*Polish Geological Institute – National Research Institute, Lower Silesian Branch, al. Jaworowa 19, 50-122 Wrocław, Poland*

Kowalski, A., Makoś, M. & Pitura, M., 2018. New insights into the glacial history of southwestern Poland based on large-scale glaciotectonic deformations – a case study from the Czaple II Gravel Pit (Western Sudetes). *Annales Societatis Geologorum Poloniae,* 88: 341–359.

Abstract: This paper presents the results of structural and sedimentological studies carried out in the outcrops of Quaternary (Middle Pleistocene) deposits near the village of Czaple in Lower Silesia, Western Sudetes. Fluvial sands, gravels and glacial tills traditionally assigned to the Middle Polish Pleistocene Glaciations (Odranian Glaciation) crop out in the active gravel pit Czaple II. In these deposits, the authors have recognised and documented numerous mesoscale glaciotectonic deformation structures that were previously undescribed from the mountainous part of the Sudetes. These structures represent effects of sediment deformation in both proglacial and subglacial settings, and include such features as asymmetrical and disharmonic folds, thrusts, steeply inclined reverse faults, normal faults and conjugate sets of fractures. Based on the orientation of kinematic indicators associated with the faults and fracture planes (slickensides, hackles, grooves, R-shears) within the fine-grained sediments and in sands and gravels, an S- and SE-directed horizontal compression due to ice-sheet advance is postulated. This direction is consistent with some relevant other data from the Sudetes, indicating that the Odranian ice sheet advanced into the area of the Sudetes from the north, north-east and north-west.

Key words: Glaciotectonic deformation, Odranian Glaciation, kinematic indices, Lower Silesia.

Manuscript received 29 October 2018 accepted 22 December 2018

INTRODUCTION

Glaciotectonic structures are widely recognized and well-documented features found in the geological substrate, whether soft sediment or bedrock, deformed by ice-sheet advances (e.g., Banham, 1977; Aber *et al*., 1989; Lee and Phillips, 2013; Phillips, 2018). These widespread and often spectacular features have been a subject of intense geological and geomorphological investigations since the 19th century (Lyell, 1863; Johnstrup, 1874; Slater, 1926), with the recognition of their geometrical similarities to large-scale, thin-skinned tectonic structures formed by crustal shortening, as in fold and thrust belts (cf. Banham, 1975, 1988; Aber, 1982; Croot, 1987; Pedersen, 1987; Van der Wateren, 1995; Phillips and Lee, 2011; Lee *et al*., 2013, 2017; Phillips *et al*., 2017). Glaciotectonic deformation structures have been described mainly from areas that were glaciated during the Pleistocene ice-sheet advances, but many analogous structures have also been reported from Palaeozoic (e.g., Rocha-Campos *et al*., 2000; Girard *et al*., 2015) and even Precambrian rocks that were influenced by ancient glaciations (Edwards, 1978). The origin and evolution of glaciotectonic deformation structures have been the subject of numerous worldwide discussions (e.g., Banham, 1975; Aber, 1982; Van der Wateren, 1985; Croot, 1987), including Polish literature (Rotnicki, 1976; Jaroszewski, 1991; Krysiak, 2007; Włodarski, 2009). Although controversies persist and there are various models for the development of these structures, it is widely accepted that glaciotectonic features are among the most useful indicators of ice-push directions that may aid spatial-temporal reconstructions of the glacier-advance stress conditions and patterns of ice dynamics (e.g., Ehlers, 1990; McCarroll and Rijsdijk, 2003; Pedersen, 2005; Aber and Ber, 2007; Lee *et al*., 2013; Dove *et al*., 2017; Phillips *et al*., 2017; Roman, in press).

Glaciotectonic structures in Quaternary deposits have been described from many sites in Poland, especially from the Polish Lowlands in the country's northern to central part (e.g., Ruszczyńska-Szenajch, 1985; Urbański, 2002, 2007; Ber *et al*., 2004; Włodarski, 2009; Widera, 2018; Roman, in press), and constitute the most common structural and morphological effect of the Scandinavian Ice-Sheet advances. A summary of the current state of knowledge on large-scale glaciotectonics in Poland is the monograph edited by Ber (2004) and the Glaciotectonic Map of Poland (Ber, 2006). In the area of Lower Silesia, SW Poland, glaciotectonic disturbances have been described in detail from only a few outcrop sites, mainly in the Sudetic Foreland (Mierzejewski, 1959; Wójcik, 1960; Jahn, 1960; Krzyszkowski and Czech, 1995; Krzyszkowski, 1996; Urbański, 2009; Urbański *et al*., 2011). Current opinions are that the vertical extent of these disturbances does not exceed the depths of 200 m in the northern part of Lower Silesia (Badura and Przybylski, 2002) and ca. 50 m in its southern part (Ber *et al.*, 2004). The spatial and vertical extent of these phenomena is little known in the mountainous southern part of Lower Silesia – the Sudetes area – where glaciotectonic features have been documented from only a few small artificial exposures and single outcrops not exceeding 3 m in height. Documentation includes several papers on small-scale glaciotectonic structures at the top of varved clays in a brickwork in Jelenia Góra, Western Sudetes (Dumanowski, 1961; Jahn, 1976; Wójcik, 1985); a description of glaciotectonic disturbances in small outcrops in the vicinity of Chwaliszów in the Wałbrzych Upland of Central Sudetes (Krzyszkowski and Stachura, 1998); and a cursory mention of glaciotectonic deformation at a poorly specified locality in the vicinity of Wojcieszów in the Kaczawa Mountains of Western Sudetes (Ber *et al*., 2004). Features of possible glaciotectonic or permafrost origin were described by Krygowski (1952) from the Wał Okmiański area in the Kaczawa Upland of Western Sudetes, about 10 km to the north from the present study site. Urbański *et al.* (2011) described Pleistocene glaciotectonic disturbances of Cretaceous sedimentary rocks in the Bolesławiec and Węgliniec area of the Izera Upland in Western Sudetes. No other examples of glaciotectonic deformation have thus far been reported from the mountainous parts of the Sudetes.

The present paper reports on previously undescribed large-scale glaciotectonic deformation features in the Pleistocene deposits of the Odranian (Saalian) Glaciation at the Czaple II Gravel Pit in the Kaczawa Foothills of Western Sudetes. Structural kinematic indicators are used to determine the local direction of ice-sheet horizontal compression. The study contributes to a better understanding of the regional palaeogeography and spatial dynamics of the Odranian ice-sheet advance in the Sudetic region of SW Poland.

GEOLOGICAL AND GEOMORPHOLOGICAL SETTING

The Czaple II Gravel Pit is located in the Lower Silesia region of SW Poland, between the towns of Złotoryja and Lwówek Śląski, at the elevation of 250–270 m a.s.l. (Fig. 1A). In the regional physical-geographical subdivision of Poland (Kondracki, 2002), this region is in the central part of the Kaczawa Foothills, Western Sudetes. The outcrop vicinity is characterized by a hilly landscape with the elevation ranging from 220 m a.s.l. (Osownia valley in Skorzynice) to 343 m a.s.l. (Kopka hill near Czaple). The gravel pit is located on an elevated denudation plain (270–300 m a.s.l.) with gently inclined slopes, dissected by stream valleys up to 20 m deep and trending WNW–ESE and W–E (see arrows in Fig. 1A). To the north, west and east from the pit, some elongate linear or arcuate ridges stand above the denudation plains to an altitude from 270 m (area of Nowa Wieś Grodziska) to over 308 m a.s.l. (vicinity of Bielanka). The length of these ridges is 0.5 to 2 km and their width is 50–200 m. The ridges are separated by parallel or subparallel depressions.

Apart from the Recent fluvial sediments and slope talus, the Quaternary deposits in the study area comprise Middle Pleistocene fluvial sand, gravel and locally silty glacial till (Przybylski *et al*., 2009) with a bulk thickness of up to 30–40 m (Milewicz and Jerzmański, 1959; Milewicz, 1961). The deposits cover a vast part of the Kaczawa Foothills in the vicinity of Czaple and are exploited in two gravel pits to the west of the village (Fig. 1B). Although not dated precisely, these deposits are generally considered to be a sedimentary residuum of the Odranian (Saalian) Middle Polish Glaciation, presently correlated with the Marine Isotope Stage 6 (MIS 6, 243–191 ka BP; Lindner and Marks, 2012).

The Odranian ice sheet, advancing from Scandinavia, covered nearly two-thirds of the Poland territory, except for its Carpathian south-eastern part (Gradziński *et al*., 2014; Marks *et al*., 2016). The areal extent of the Odranian ice sheet in south-western Poland is generally assumed to have reached the northern slopes of the Sudetic Mountains and it has been suggested that the ice-sheet front formed several topographically controlled lobes when invading the areas

Fig. 1. Location of the study area. **A**. Morphological map of the Czaple area generated from LiDAR elevation data. The red square indicates location of the Czaple II Gravel Pit and the white arrows point elongate arcuate topographic ridges of Quaternary deposits. **B**. Upper part: Location of the study area in Poland. Lower part: Simplified sketch-map of the Czaple II Gravel Pit with outcrop localities 1–5 referred to in the text. **C**. Distribution of Quaternary deposits in the Czaple area in relation to bedrock geology; simplified and slightly modified compilation from Sztromwasser (1995), Badura (2005), Cymerman *et al*. (2005) and Kozdrój *et al*. (2005). Explanations of letter symbols: KMC – Kaczawa Metamorphic Complex; NSS – North Sudetic Synclinorium; JF – Jerzmanice Fault; SMF – Sudetic Marginal Fault.

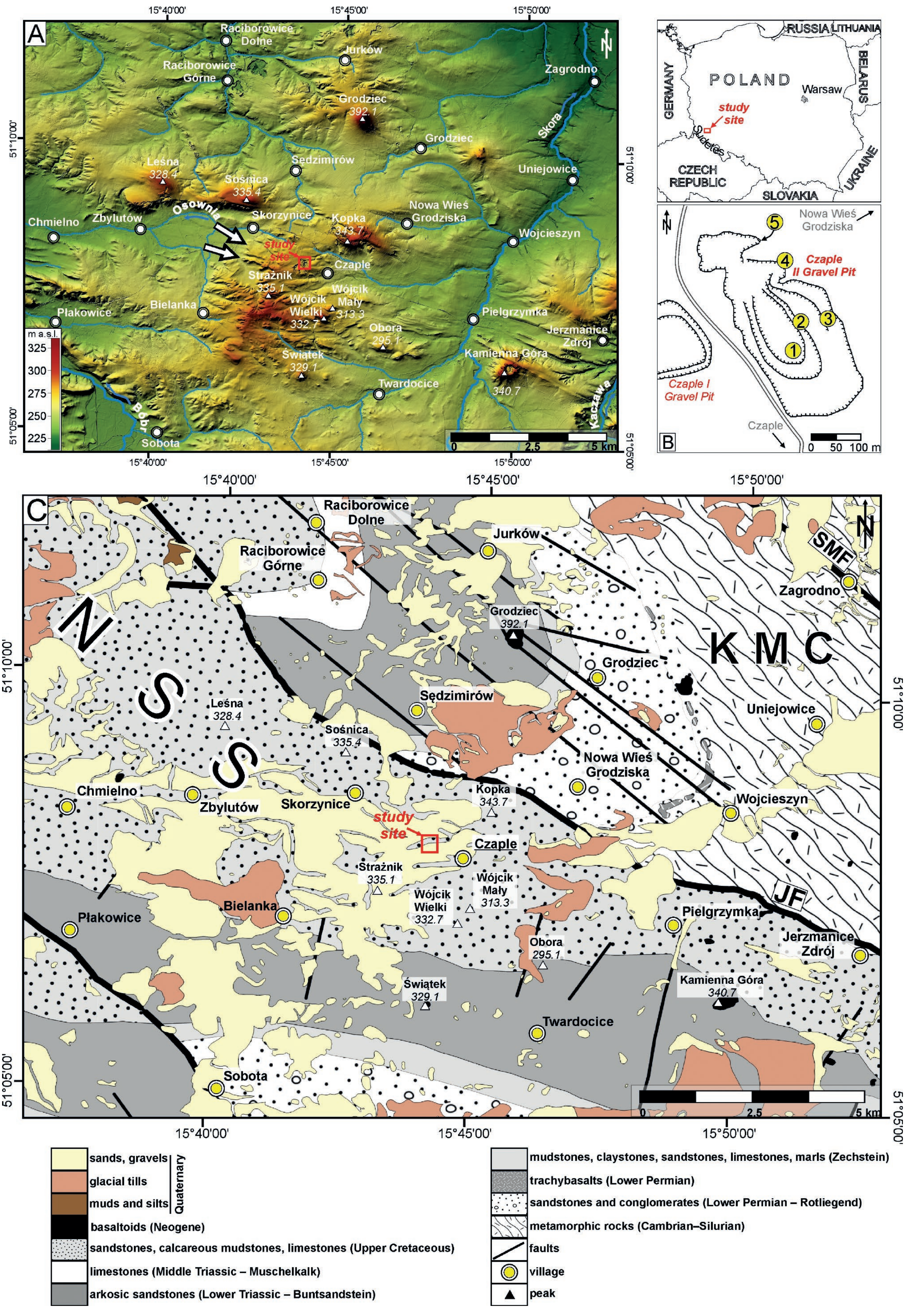
A
B
C
POLAND
Warsaw
GERMANY
RUSSIA
LITHUANIA
BELARUS
UKRAINE
SLOVAKIA
CZECH REPUBLIC
Sudetes
study site
Nowa Wieś Grodziska
Czaple II Gravel Pit
Czaple I Gravel Pit
Czaple
0 50 100 m
m a.s.l.
325
300
275
250
225
0 2.5 5 km
Osownia
Skora
Bóbr
Kaczawa
Raciborowice Dolne
Raciborowice Górne
Jurków
Zagrodno
Grodziec 392.1
Grodziec
Leśna 328.4
Sośnica 335.4
Sędzimirów
Uniejowice
Chmielno
Zbylutów
Skorzynice
Kopka 343.7
Nowa Wieś Grodziska
Wojcieszyn
Czaple
Strażnik 335.1
Wójcik Wielki 332.7
Wójcik Mały 313.3
Bielanka
Płakowice
Pielgrzymka
Jerzmanice Zdrój
Obora 295.1
Świątek 329.1
Kamienna Góra 340.7
Twardocice
Sobota
NSS
KMC
SMF
JF
15°40'00'
15°45'00'
15°50'00'
51°10'00'
51°05'00'
sands, gravels
glacial tills
muds and silts
Quaternary
basaltoids (Neogene)
sandstones, calcareous mudstones, limestones (Upper Cretaceous)
limestones (Middle Triassic – Muschelkalk)
arkosic sandstones (Lower Triassic – Buntsandstein)
mudstones, claystones, sandstones, limestones, marls (Zechstein)
trachybasalts (Lower Permian)
sandstones and conglomerates (Lower Permian – Rotliegend)
metamorphic rocks (Cambrian–Silurian)
faults
village
peak

of the present-day Kaczawa and Izera foothills (Wójcik, 1985; Badura and Przybylski, 1998), but the exact palaeogeographic extent of the ice sheet remains to be poorly documented. Therefore, all new pieces of field evidence, such as the present study, are highly valuable to this regional knowledge.

In the present study area near Czaple (Fig. 1A, B), the Pleistocene deposits rest unconformably on the bedrock assigned to the North Sudetic Synclinorium (NSS) and the Kaczawa Metamorphic Complex (KMC) (Fig. 1C). These pre-Cenozoic geological units at the north-eastern terminus of the Bohemian Massif are in the northern part of the Sudetic Block, which is an elevated complex horst structure bounded to the north by the Sudetic Marginal Fault from the down-thrown Fore-Sudetic Block (Żelaźniewicz *et al*., 2011). In the study area, the KMC rocks are unconformably overlain or tectonically covered by the NSS sedimentary rocks (Fig. 1C; see Cymerman, 2004).

The KMC consists of metasedimentary and metavolcanic rocks that were strongly folded, faulted and weakly metamorphosed (lower/middle greenschist facies) during the Variscan orogeny (Baranowski et al., 1990; Kryza and Muszyński, 1992; Cymerman, 2002; Żelaźniewicz *et al*., 2011). The rocks are of Cambrian to Early Carboniferous age and include mainly phyllites, sericite schists, metasandstones, metamudstones, metalydites and crystalline limestones to marbles, as well as rocks that originated due to submarine volcanism and plutonism: pillow-lava metabasalts, basaltic tuffs, metarhyolites, metarhyodacides, metadolerites and metagabbros.

The NSS formed by the end-Cretaceous folding and faulting of the sedimentary-volcanic infill of the North Sudetic Basin, a post-Variscan sedimentary basin developed in the late Carboniferous (Teisseyre *et al*., 1957; Baranowski *et al*., 1990; Śliwiński *et al*., 2003). The basin-fill comprises terrestrial to shallow-marine sedimentary rocks (Raumer, 1819; Scupin, 1913; Milewicz and Górecka, 1965; Górecka, 1970; Mroczkowski, 1972; Milewicz, 1985, 1997; Wojewoda and Mastalerz, 1989; Raczyński, 1997; Chrząstek, 2002; Chrząstek and Wojewoda, 2011; Solecki, 2011; Leszczyński, 2018) and includes Early Permian and Neogene volcanics (Kozłowski and Parachoniak, 1967; Awdankiewicz, 2006).

The KMC and NSS bedrock in the study area is dissected by faults trending NW–SE and NE–SW, forming a system of horsts and grabens (Fig. 1C; Scupin, 1913, 1933; Beyer, 1933; Teisseyre *et al*., 1957). One of the most prominent faults in the NSS near Złotoryja is the Jerzmanice Fault that trends WNW–ESE, cuts the northern slopes of the Kopka hill to the north of Czaple (Fig. 1C) and separates rocks of different ages. Neotectonic activity of the Jerzmanice Fault and the Sudetic Marginal Fault in the vicinity of Złotoryja was inferred from morphometric analyses (Mastalerz and Wojewoda, 1990; Migoń and Łach, 1999; Badura *et al*., 2007).

METHODS

The present study, carried out in the Czaple II Gravel Pit in 2017–2018, was focused on the description and measurement of structural glaciotectonic features in the Quaternary deposits. The deposits were macroscopically described and logged in the field with the use of standard sedimentological techniques and lithofacies codes (Miall, 1985; Zieliński and Pisarska-Jamroży, 2012). The textural and structural features of individual sedimentary units were used to interpret primary depositional processes and palaeoenvironment. Palaeoflow directions were reconstructed from sedimentary indices, taking into account the effects of glaciotectonic deformation.

The recognition and description of deformation structures required detailed structural analysis combined with sedimentological and petrographical investigations. Measurements involved the spatial attitude of main structural surfaces and indices of ice-flow directions. These indices included mainly compressional deformation mesostructures created by ductile and brittle deformation (cf. Phillips, 2018): cylindrical and non-cylindrical folds, low-angle thrusts, both reverse and normal faults, sets of fractures, deformation bands, zones of brecciation as well as structures linked with hydroplastic sediment behaviour (such as diapirs, injection structures and dewatering structures). Structural mapping involved the recognition of joints and fault planes. Mesostructural kinematic indicators, such as striated ridges, grooves, slickensides, low-angle shears, hackles and *en echelon* cracks (Petit, 1987), were carefully identified and measured. Measurements of the position of structural planes were made with a conventional geological compass with an accuracy of ± 2° and were supplemented by measurements with the use of the FieldMove Clino mobile application developed by Midland Valley. Special attention was given to the exact location and spatial extent of deformation by using precise GPS receivers. The measurements of all structural features are presented on great circle diagrams, pole point diagrams and contour diagrams with projection on the lower hemisphere of the Schmidt-Lambert stereonet.

In addition, the orientation of clast long axes clast (clast fabric) was measured in an outcrop of grey diamicton tills exposed in the northernmost part of the pit in 2017. These measurements were derived from several small exposures (max. 5 m x 2 m) and included 80 cobbles with the longest axis of 4–12 cm (Wachecka-Kotkowska, 2015). The data were plotted on stereonet as contour diagrams.

STUDY RESULTS

Sedimentology and provenance of the Pleistocene deposits

The deposits exposed in the gravel pit are cross-stratified sands and gravels, interpreted earlier as fluvioglacial and attributed to the Odranian (Saalian I) Glaciation (Milewicz and Jerzmański, 1959). The thickness distribution and areal extent of these deposits were recognized through the primary geological documentation work for the Czaple open-pit mine (Jarecki, 2009), when many shallow boreholes were drilled in the area. The data indicate a total thickness of the deposits of up to ca. 30 m and show that they are both overlain and underlain by two distinct horizons of glacial till (see the lowermost and the uppermost till in Fig. 2). The lowermost glacial till is not exposed in the pit, but was found beneath the sand and gravel deposits in several bore-

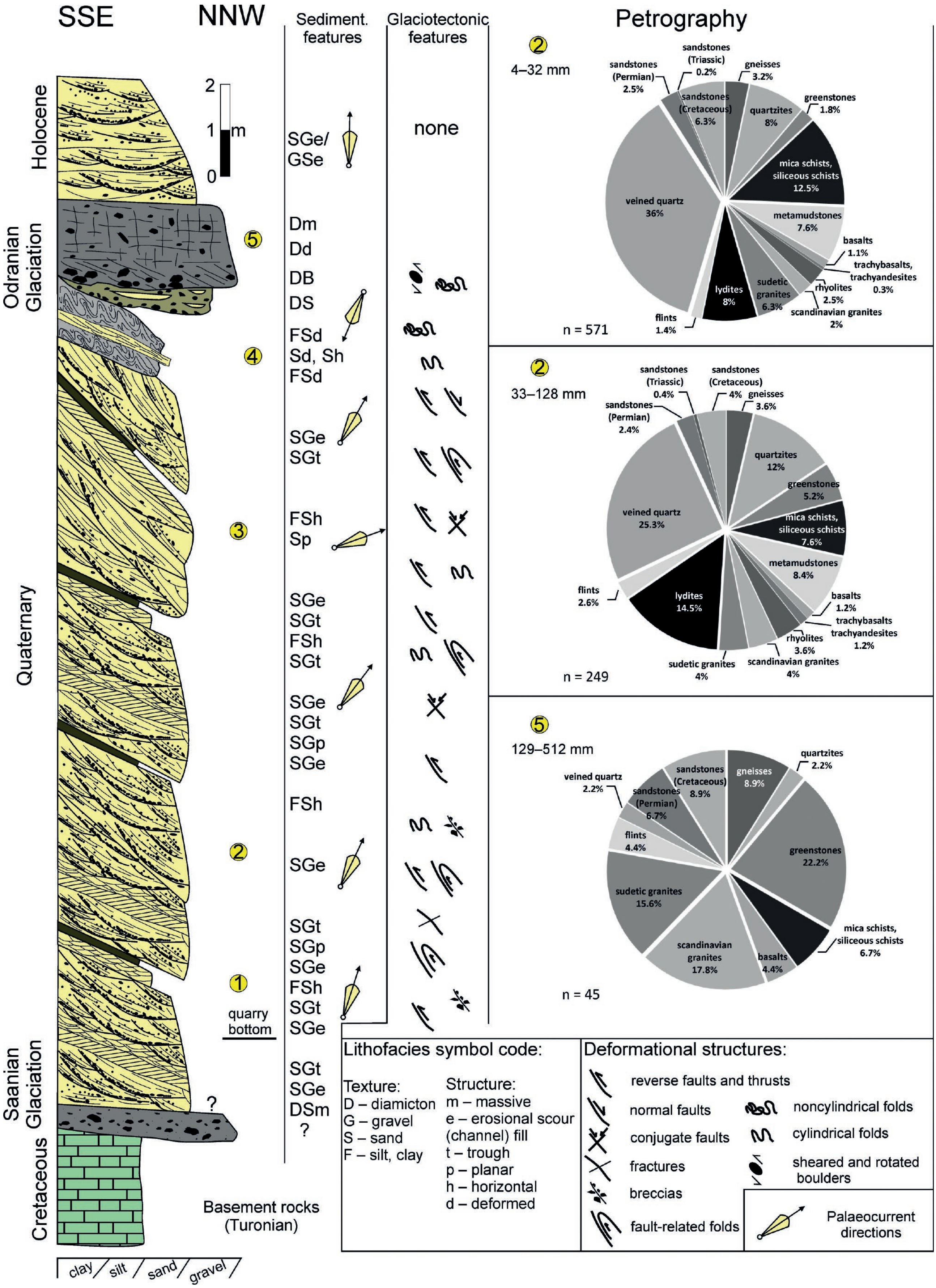

Fig. 2. Synthetic sedimentary profile of Quaternary deposits in the Czaple II Gravel Pit, compiled from outcrop localities 1–5 (Fig. 1B). Indicated are main component sedimentary facies (letter code as the text), glaciotectonic features and lithological composition of gravel clasts (percentage data from localities 2 and 5).

holes (Jarecki, 2009). This till rests unconformably on an Upper Cretaceous bedrock (calcareous mudstones and claystones assigned to the middle Turonian; Milewicz, 1997) and is probably a relic of the Elsterian Glaciation (Sanian II, MIS12). The uppermost glacial till covers unconformably the sand and gravel deposits exposed in the gravel pit and most probably represents the Saalian Glaciation (Odranian, MIS 6).

Representative outcrop logs of the sand and gravel deposits, from localities 1–3 (Figs 1B, 2), show fining-upwards lenticular packages, 2 m to 4 m thick, composed of sheet-like beds that are 0.3 to 2 m thick and have a lateral extent of up to 5 m (Fig. 3A). The lower and upper bed boundaries are mainly sharp (erosional), less often gradational. The lower parts of bed sets consist typically of a moderately sorted, fine- and medium-grained (MPS ≈ 12 cm), clast-supported gravel (facies Gm) that passes gradationally upwards into large-scale cross-stratified sand. Sand contains scattered well-rounded pebbles up to 5 cm in length and its cross-strata are inclined at ca. 15–20° towards the W and SW as the infill of asymmetrical trough-shaped erosional scours (facies SGe). The stratification is commonly deformed, with the main bedding surfaces showing a secondary inclination of 45° to 90° (Fig. 3A). The cross-stratified pebbly sand passes upwards into a finer-grained sand with planar (facies SGp) and trough cross-stratification (facies SGt; Fig. 3B), commonly covered by a weakly flat-laminated or structureless (facies Fsd) fine-grained deposit (sandy mud, mud or clay) up to 0.2 m thick.

This part of the sedimentary succession, with the fining-upwards bed packages, is interpreted as the deposits of laterally unstable, cut-and-fill braided fluvial channels. The gravel is apparently a channel lag and the inclined beds of sandy gravel and cross-stratified sand are interpreted as deposits of superimposed, offset-stacked braid bars, while the muddy to clayey capping represents channel abandonment. The measured approximate direction of these palaeochannels and their internal flow-direction indices suggest sediment transport from the SW and subordinately from the WSW (Fig. 2).

In the middle part of the pit (locality 4, Figs 1B, 2), this succession of gravel and sand is unconformably overlain by diffusely laminated or structureless, strongly folded, alternating muddy and silty deposits (facies FSd) with sporadic intercalations of sand (facies Sd and Sh) 0.1 to 1 m in thickness. The total thickness of this package of fine-grained deposits is ca. 2–3 m, and they are interpreted as glaciotectonically deformed glaciolacustrine sediments.

A subordinate component of the sedimentary succession are layers of grey muddy to sandy diamicton, exposed in the northern part of the pit (locality 5, Fig. 1B). The diamictons range from laminated (facies Dd) to structureless (facies Dm), contain scattered pebbles and cobbles (Fig. 3C) and cover the above described other deposits. The diamicton unit in its best-preserved part is up 2 m thick, showing a sharp and probably erosional lower contact, locally with an undulating (deformed?) wavy geometry. The lowermost part of this unit consists of a stratified, silty to sandy diamicton with cobbles up to 15 cm in size, whereas the uppermost part consists of a structureless silty to sandy diamicton. In the middle part of the outcrop, the diamicton locally passes laterally into a sandy to gravelly diamicton (facies DS) that shows no evidence of deformation. This sandy diamicton shows narrow (up to 1 m in width) erosional runnels trending N–S (Fig. 3D) and filled with a disorderly mixture of gravel clasts up to 20 cm in size.

The heterogenous diamicton package is thought to comprise layers of both subglacial till (Shilts, 1976; Eyles *et al.*, 1983; Brodzikowski and Van Loon, 1987) and superglacially derived melt-out flowtill (Hartshorn, 1958; Zieliński and Van Loon, 1999). This latter notion is supported by the evidence of non-deformed diamicton layers and by the occurrence of gravel-filled erosional water runnels within the diamicton package, which may jointly indicate local ice-front oscillations.

Gravel clasts over 4 mm in size were collected from the fluvioglacial succession and the overlying till unit for a petrographic and provenance analysis (Fig. 2). Two such samples from the lower part of fluvioglacial deposits comprised, respectively, 571 clasts of pebble size up to 32 mm in length and 249 clasts of pebble to small-cobble size up to 128 mm in length. A third sample, from the diamictic upper part of the succession, comprised 45 clasts of pebble to boulder size, up to 512 mm in length.

Most of the fluvioglacial gravel (>90%) appeared to be of a local provenance, although the percentage of various components varied with the clast size (Fig. 2). The most common components (25.3–36%) are vein quartz and clasts derived from the KMC bedrock assemblage (sericite schists, metamudstones, metalydites, greenstones and quartzites). The second group of components are fragments of the NSS bedrock, including its Permian sandstones (up to 2.5%) and volcanic rocks (rhyolites 2.5–3.6%, trachyandesites and trachybasalts 0–1.2%), Permo-Triassic sandstones (0.2–0.4%) and Cretaceous sandstones (4–6.3%), with a small admixture of Cenozoic basalts (1.1–1.2%). Notable is the contribution of rock debris derived from the adjacent geological units, such as the Izera gneisses (3.2–3.6%) and the Karkonosze and Strzegom-Sobótka granitoids (4–6%). Erratic clasts are rare, represented by the Scandinavian Rapakivi granites (up to 4%) and the Jurassic or Cretaceous cherts (1.4–2.6%) derived probably from the northern Polish Lowlands.

The overlying glacial till unit similarly contains mainly local rock debris: greenstones (up to 22%), mica and siliceous schists (6.7%), quartzites (2.2%) and vein quartz (up to 2.2%), derived from the KMC. Relatively more abundant are erratic Scandinavian granitoids (17.8%) and cherts from Polish Lowlands (4.4%). Richer represented are also Sudetic granitoids (15.6%) from the Karkonosze and Strzegom-Sobótka massifs, as well as gneisses (8.9%) derived probably from the Karkonosze–Izera Massif. Admixture of local non-metamorphic rocks includes Cretaceous (8.9%) and Permo-Triassic sandstones (6.7%) as well as Cenozoic basalts (4.4%) derived from the NSS area.

Glaciotectonic deformation

Three main types of macroscopic glaciotectonic structures have been recognized in the Czaple II Gravel Pit:

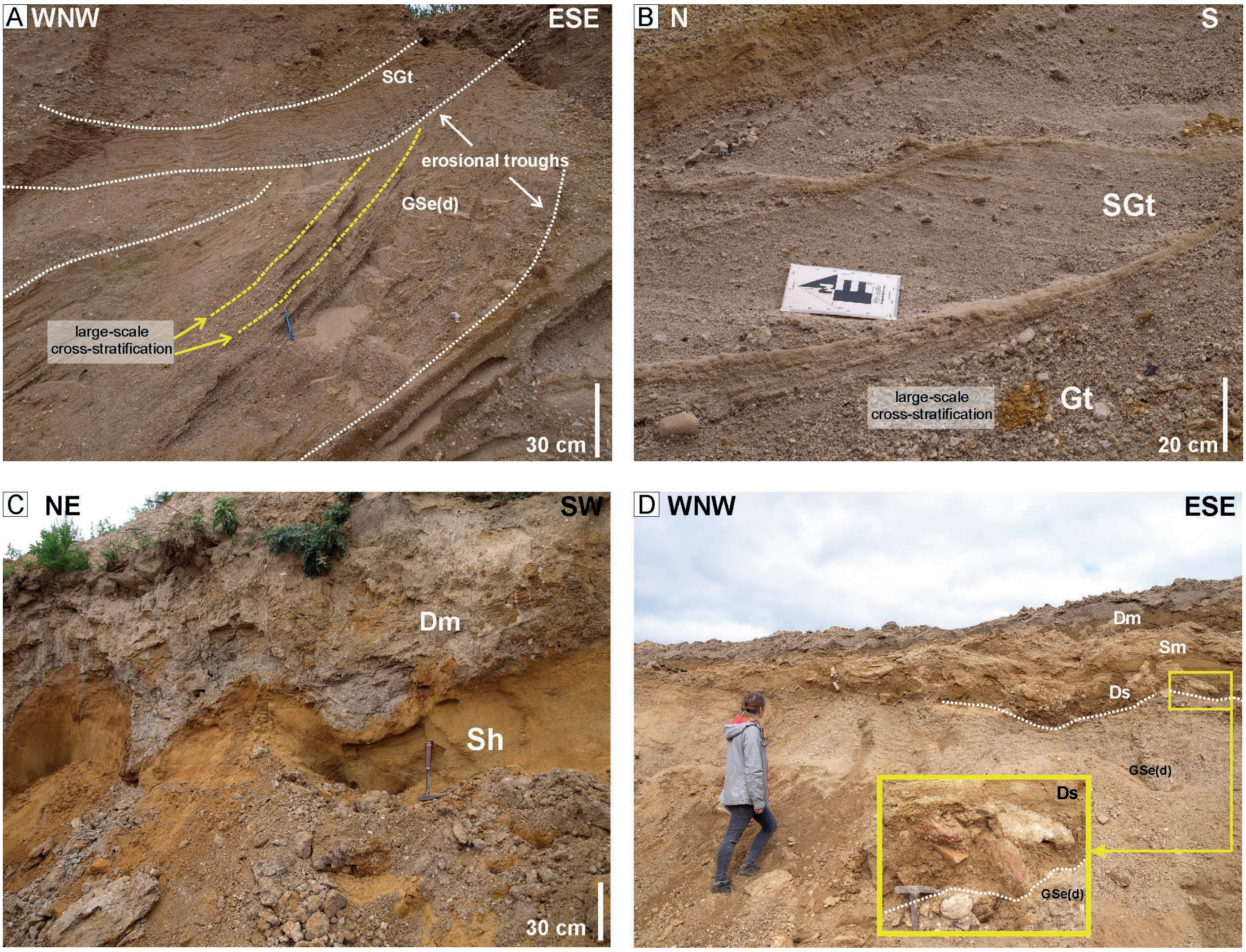

Fig. 3. Sedimentary and structural features of Pleistocene deposits in the Czaple II Gravel Pit. **A**. Large-scale cross-stratification in sand and gravel (lithofacies SGt and GSe) at locality 3, associated with asymmetrical erosional troughs (white dashed lines) trending NNE–SSW. Deposits tilted by glaciotectonic deformation. **B.** Cross-stratified pebbly sand (facies SGt/SGp) underlain by cross-stratified gravel (facies Gt) at locality 2. **C.** Undulating, deformed basal contact of the upper till unit (massive diamicton, facies Dm) at locality 5. The underlying deposits are fine-grained, horizontally stratified sands (facies Sh). **D.** Composite sandy till (facies Ds, Sm and Dm) at locality 3, with its base (white dashed line) showing narrow scours up to 1 m wide and trending N–S orientation. The scours are filled with disorganized cobble to boulder gravel (see inset close-up detail).

– strongly dislocated and imbricated thrust sheets composed of fluvial gravel and sand and bounded by steeply inclined reverse faults or thrusts, with such internal secondary structures as reverse or normal dip-slip faults and fault-related folds from centimetres to several metres in size as well as sets of conjugate fractures, tectonic breccias and diapirs.
– asymmetrical, cylindrical to non-cylindrical folds, subordinately disharmonic, as well as sheath folds, found only in the fine-grained argillaceous deposits in the northern part of the pit.
– shear structures observed in the lowermost part of the glacial till unit and – like the fold structures – representing typical ductile deformation.

Faults and associated structures

The main structural features observed in the pit outcrop (localities 1–3, Fig. 1B) are reverse faults and thrusts that bound thrust-sheet slices (Fig. 4A, B). The thickness of individual thrust sheets ranges from 0.3 to ca. 4 m. Reverse faults and thrusts show mainly listric or planar geometry (Fig. 4C) and are concordant or striking obliquely to the main bedding surfaces. The fault planes of thrusts show ENE–WSW and NE–SW strike trends and a dip of 10–30° towards the NNW and NW, respectively. Reverse faults are steeper, inclined at 45-80° towards the NW, and show an ENE-WSW strike trend. The offset along the main thrust planes is estimated roughly at 4 to 5 m, but is difficult to measure exactly due to the lack of recognizable marker horizons in the sliced deposits. The amount of total displacement can be determined solely on the surfaces of small-scale thrusts and reverse faults, and apparently does not exceed 2 m.

It is worth mentioning that reverse faults at localities 1–3 (Fig. 1B) occur frequently in the fine-grained argillaceous intercalations within the sand-gravel unit (Fig. 4C). Sub-vertical fault planes developed in these sediments are

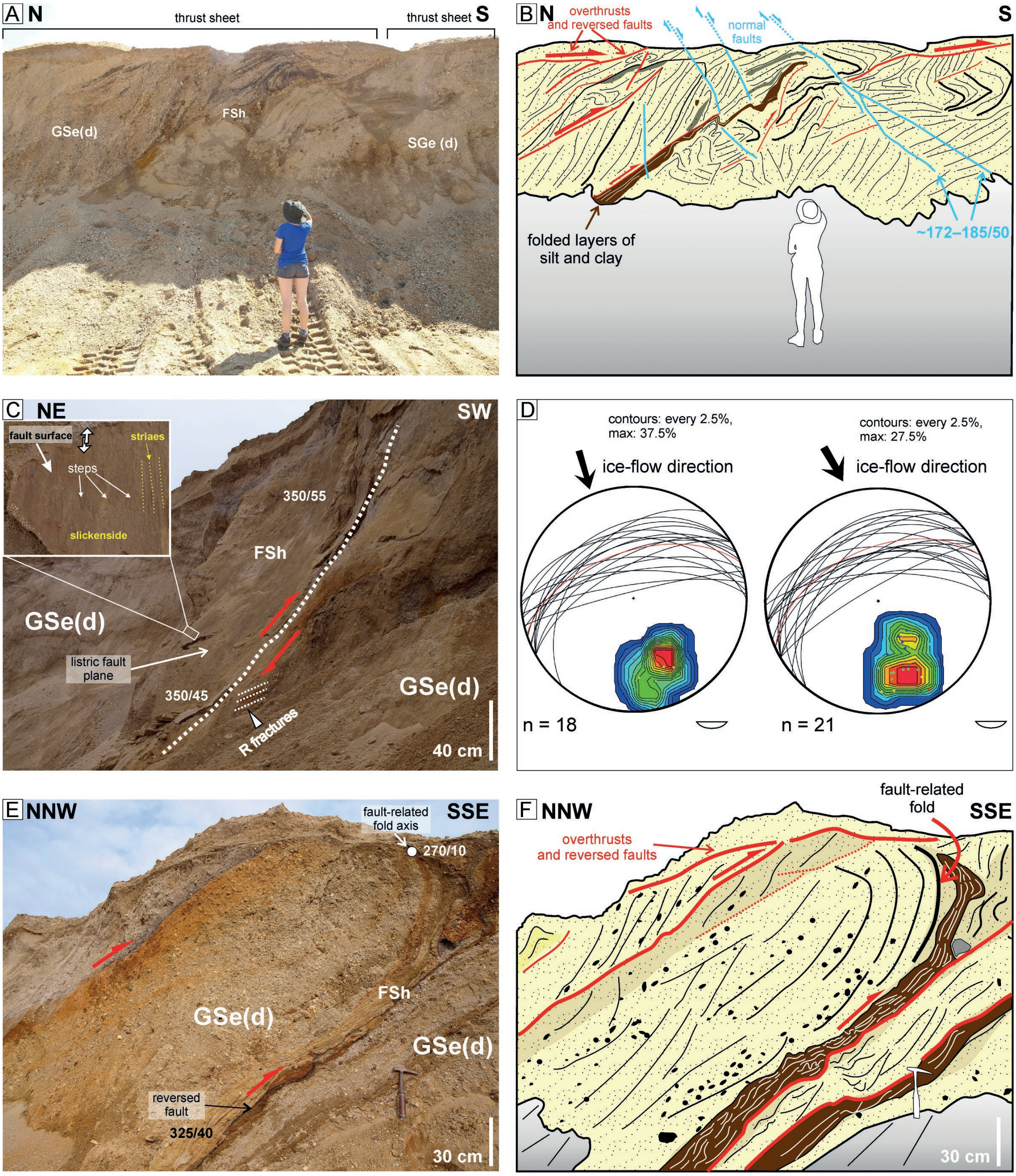

Fig. 4. Reverse faults and thrust sheets in the Czaple II Gravel Pit at localities 1 and 2. **A**, **B.** Outcrop photograph with an interpretive sketch showing NW- and NNW-dipping reverse faults and thrusts bounding thrust-sheet slices. Thrust-sheet boundaries are mainly in silty and clayey sediments (brown). Note that reversed faults are cut and displaced by normal dip-slip faults (blue). **C.** Reverse fault developed within silty to clayey deposits in the lower part of the pit. The listric fault plane is strongly polished and striated, showing slickensides and steps (see inset close-up detail). Visible also are low-angle R-shears (white lines) associated with the fault surface. **D.** Stereoplots (pole-point great-circle contour diagrams) of the orientation of reversed fault (left) and bedding surfaces (right) within fluvioglacial deposits. The arrow indicates interpreted direction of ice-sheet movement (compression). **E**, **F.** Outcrop photograph and interpretive sketch of a fault-propagation fold (hanging-wall anticline) developed above the NW-dipping surface of reverse fault (red line).

strongly polished and striated, especially in the lower part of the pit. They dip at 45–70° towards the NW (Fig. 4D) and show slickensides, striae and steps that clearly indicate a reverse sense of movement (Fig. 4C). Low-angle R-shears are associated with the fault surfaces in some cases (Fig. 4C). In contrast, fault surfaces formed within sand and gravel are not well visible, merely highlighted by thin zones of secondary silicification and enrichment in iron- and manganese-oxides (deformation bands; cf. Fossen *et al*., 2007). These zones range from a few centimetres to 0.3 m in thickness. Minor fault-related secondary features include narrow breccia zones that occur both above and below the fault surface. They are manifested as strongly fractured and sheared sets of clustered boulders that form apparent gravel lags.

Locally observed at locality 1 (Fig. 1B) are minor folds related to fault surfaces (Fig. 4E, F). They involve fault-propagation folds and fault-bend folds with gently inclined axes trending W–E. Fault-propagation folds occur particularly near the bottom of the pit, where hanging-wall anticlines developed in association with main thrust surfaces. These SE-verging anticlines formed above the planar or listric surfaces of inverse faults dipping at 45–80° to the NW.

The sand-gravel deposits at localities 1–3 (Fig. 1B) show also single or conjugate sets of normal dip-slip faults (Fig. 5). These normal faults, striking W–E or WNW–ESE, cut across and displace thrust sheets as well as their bounding surfaces of reverse faults or thrusts (Fig. 5A, B, F). The surfaces of the normal faults are typically planar or curved (listric) and dipping at 45–90° towards the S or more commonly to the SSW. These dip-slip faults show a throw of a few centimetres to as much as 1.5 m (Fig. 5A, B).

Other evidence of brittle deformation in the lower part of the pit are numerous normal faults striking W–E and dipping at up to 70° to the NNE, as well as smaller antithetic faults dipping to the SSW at up to 45°. Close to the fault surfaces at locality 1 (Fig. 1B) occur low-angle or even horizontal fractures (Fig. 5C, D) that show little evidence of displacement, with an offset of no more than a few millimetres. These structures and the fault surfaces are accentuated by wide zones of brecciation and enrichment in iron oxides (Fig. 5C, E).

Fold structures

Folds and related small-scale structures produced by ductile (hydroplastic) deformation of unconsolidated sediment occur mainly at locality 4 (Fig. 1B) in the northern part of the pit outcrop, where they formed in the heterogenous fine-grained deposits below the glacial till unit. Well-developed assemblages of folds were observed there in 2017, about 1–2 m below the till unit (Fig. 6). The lamination surfaces of these argillaceous deposits intercalated with sand are parallel to the till lower boundary, but strongly sheared and plastically deformed. Folds are mainly asymmetrical and recumbent, with axes trending W–E and WSW–ENE (Fig. 6A). The amplitudes of folds are up to 1 m and their axial planes are inclined at ca. 15–25° towards the NW (Fig. 6B). Interlayers of fine-grained sand (facies Sh) are frequently exposed in the crosscut sections of fold hinges. Smaller-scale parasitic folds, with an amplitude range from several millimetres to ca. 5 cm, occur in the intercalated silt and clay within the fold hinge zones (Fig. 6C). The axes of these folds are inclined towards the N or NW. Sand interlayers show tight isoclinal folds with an amplitude of ca. 0.3 m and limbs steeply inclined at 80–90° to the NW and SE (Fig. 6D).

Some of the folds in fine-grained facies FSd show a geometry typical of non-cylindrical, sheath folds formed by shearing (Fig. 6E, F). Fold axes are inclined at 5° to 35° towards the WNW or ESE, with the fold limbs inclined at varied angles toward the NW and SE. Locally observed were also eye-shaped sheath folds (Fig. 6E, F), or eye-type folds (cf. Alsop and Holdsworth, 2006), with their longest axes parallel to the NW–SE and N–S shearing directions (cf. Fossen, 2010).

Deformation structures in glacial till

Deformation structures were observed also in small outcrops of the lowermost part of the till unit (see Fig. 2) at locality 5 (Fig. 1B). This part of the unit consists of stratified, silty to sandy diamictons with cobbles up to 15 cm in size and deformed sand and silt lenses. Well-developed is shear foliation dipping at 20–45° towards the NW, with rotated pebbles and sheared cobbles plunging obliquely to the shear surfaces at an angle of up to 50° (Fig. 7A). Pronounced alignment of the long axes of scattered gravel clasts indicates shear direction towards the SE (Fig. 7A). Present also are water-escape structures as well as sand diapirs and parallel sheeted dykes, some of them fragmented and turned into ‘rolled’ sand clasts (Fig. 7B).

DISCUSSION

Glaciotectonic deformation

The observed deformation structures show a wide range of varieties and scales (Figs 3–8), which apparently reflects the lithological and rheological variability of the deformed deposits. The analysis of these structures, based on widely used conventional criteria (cf. Christiansen and Whitaker, 1976; Aber *et al*., 1989; Pedersen, 2000; Aber and Ber, 2007; Evans, 2007; Phillips *et al.*, 2008; Benediktsson *et al*., 2008; Włodarski, 2009; Phillips *et al*., 2011; Lee *et al*., 2013), allowed reconstruction of the kinematic history and physical conditions of the sediment deformation – attributed to glaciotectonics. The deposits are in their primary contact with bedrock, show no evidence of modern landslide processes and, although undated, have long been regarded as a part of the regional Pleistocene ice-age sedimentary cover (Milewicz and Jerzmański, 1959; Milewicz, 1961; Badura and Przybylski, 2002; Jarecki, 2009; Przybylski *et al*., 2009). Exotic rock-debris components derived from Scandinavia and Polish Lowlands confirm that the sediments in the study area came from the Pleistocene ice sheet (Badura and Przybylski, 1998; Przybylski *et al*., 2009). However, their glaciotectonic deformation was overlooked by previous regional studies (see reviews by Ber, 2004, 2006).

Features such as imbricate thrust-sheet fans in proglacial deposits (Figs 4, 8) are typical glaciotectonic structures representing the direct effect of ice-margin push during the glacier advance, with fine-grained argillaceous sediments

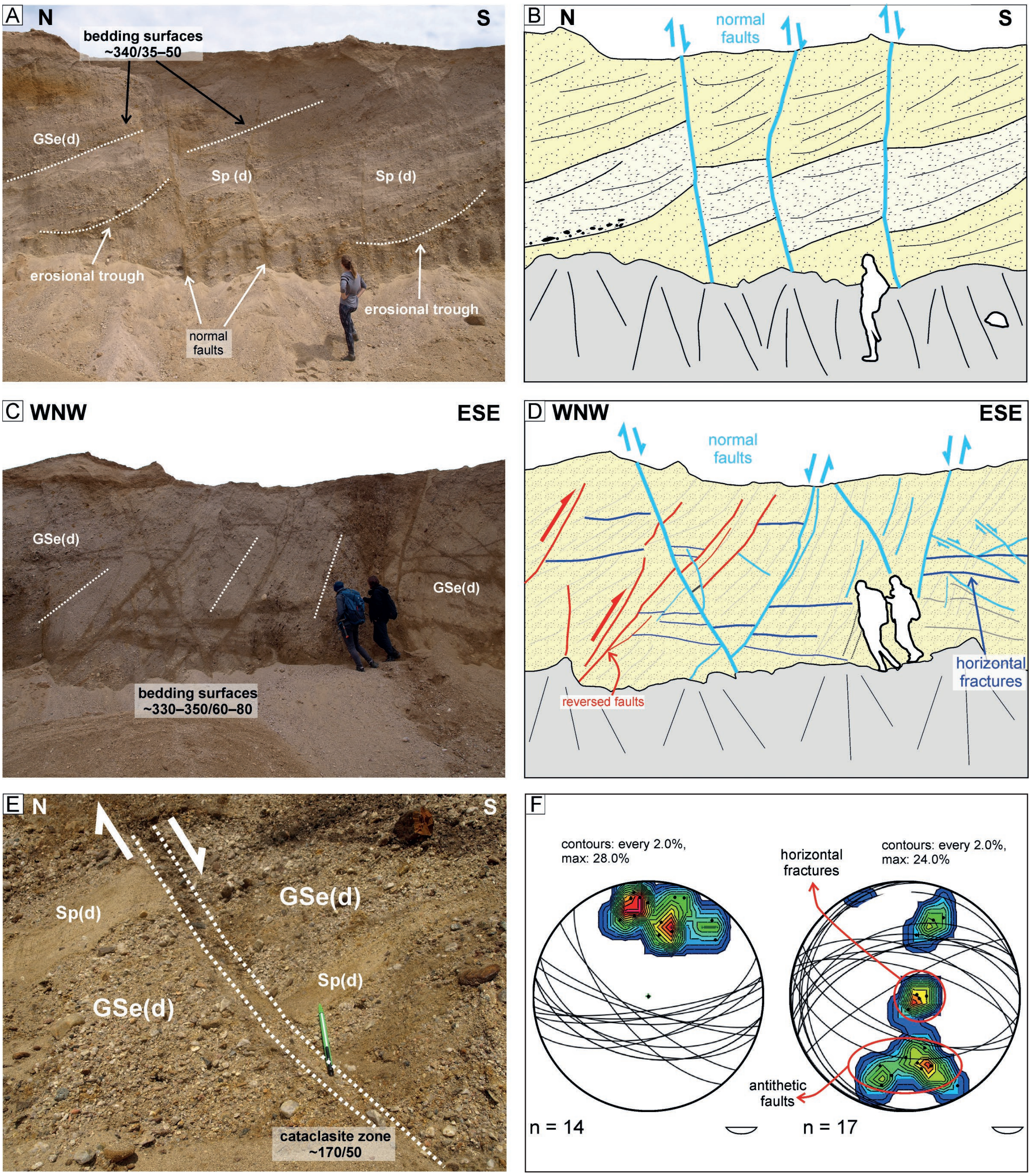

Fig. 5. Normal dip-slip faults at localities 1 and 2 in the Czaple II Gravel Pit. **A**, **B.** Outcrop photograph with an interpretive sketch showing a set of normal dip-slip faults (blue lines) with offset of up to 1.5 m. **C**, **D.** Outcrop photograph with an interpretive sketch showing normal dip-slip faults and smaller antithetic faults, trending W–E and dipping at high angle in opposite directions (mainly to the WNW). Note that close to the fault surfaces occur low-angle or even horizontal fractures with no evidence of displacement. Fault and fracture surfaces are accentuated by zones of brecciation and enrichment in iron oxides. **E.** Small-scale dip-slip fault with a few centimetre offset and an associated narrow shear-breccia zone (shear band) marked by white dotted lines. **F.** Stereoplots (pole-point great-circle contour diagrams) of the orientation of normal dip-slip fault surfaces (left) and related sets of conjugate faults and fractures (right) in glaciotectonised fluvial deposits; note antithetic faults and horizontal fractures.

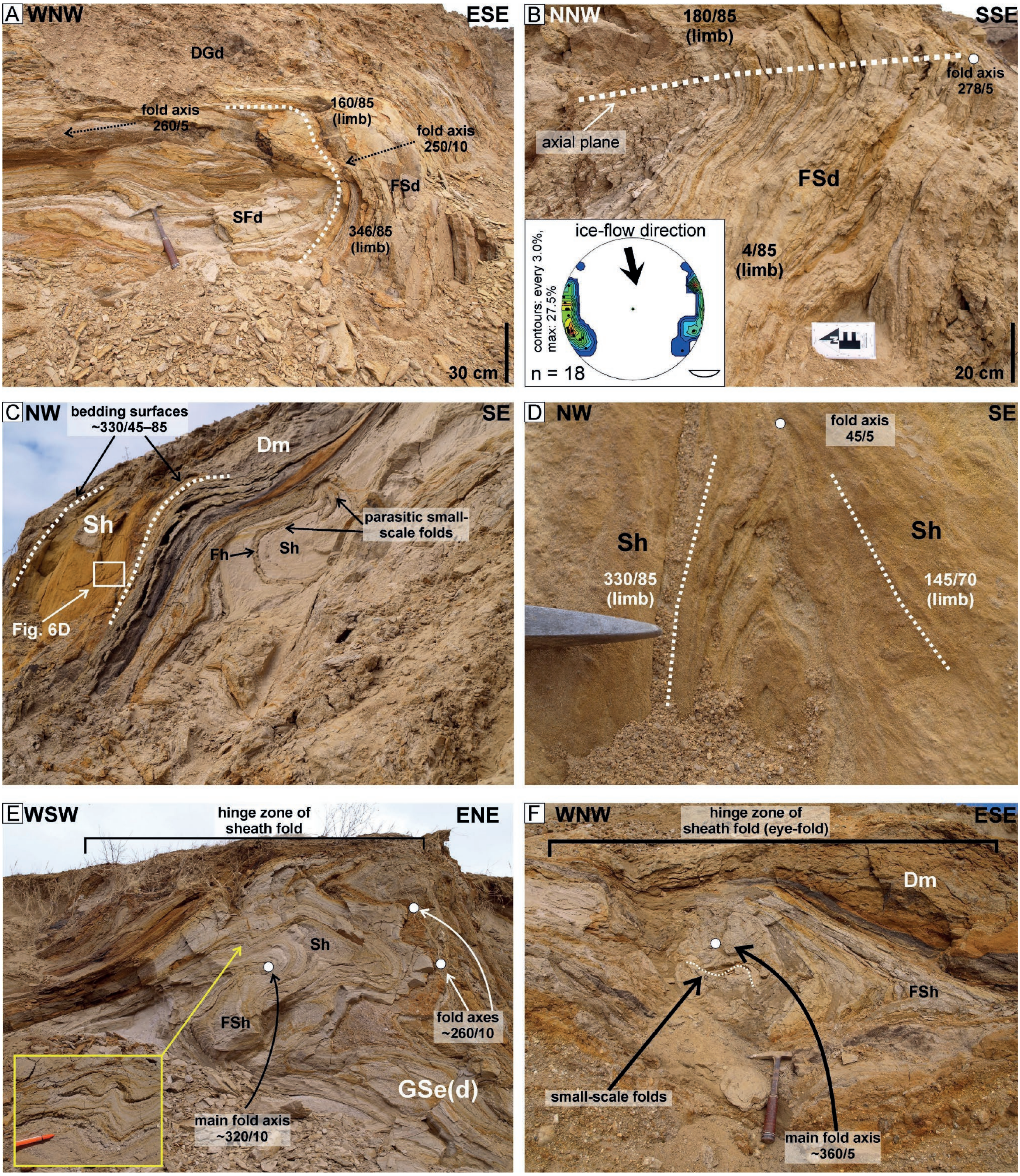

Fig. 6. Fold structures at locality 4 in the Czaple II Gravel Pit. **A.** Recumbent fold (axis trending WSW–ENE) in glaciolacustrine deposits. Note that the fine-grained sand interlayers (facies SFd) exposed within the fold hinge. **B.** Large, SSE-overturned recumbent fold in laminated laciolacustrine deposits (facies FSd) below the upper till unit. The inset stereoplot shows orientation of recumbent fold axes in glaciolacustrine deposits. **C.** Small parasitic folds in the hinge zone of a large recumbent fold. **D.** Tight isoclinal folds in planar parallel-stratified sand (facies Sh). **E.** Sheath fold with a complex geometry in fine-grained glaciolacustrine deposits (facies FSd). The main fold axis is trending NW–SE, parallel to the shearing direction towards the viewer (cf. Fossen, 2010). **F.** Cross-section through a typical sheath fold (eye-type fold, cf. Alsop and Holdsworth, 2006). The N–S fold axis is parallel to the shearing direction (towards the viewer).

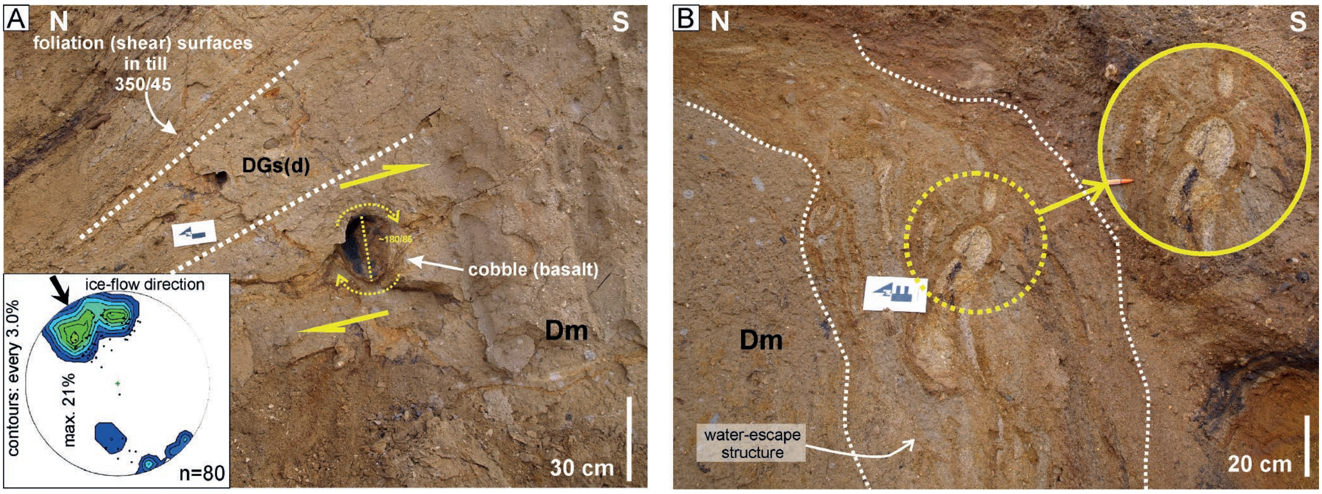

Fig. 7. Deformation structures in the lowermost part of the glacial till unit (locality 5). **A.** Deformed laminated diamicton of facies DGs(d), with scattered pebbles and cobbles, in the till unit at locality 5. Note the rotated and sheared basaltic cobble. The inset stereoplot shows measurements of the orientation of gravel clasts long axes (clast fabric) compared with the interpreted direction of ice-sheet movement. **B.** Deformation features in massive diamicton (facies Dm) at locality 5), with rolled-up sand clasts aligned within water-escape structure.

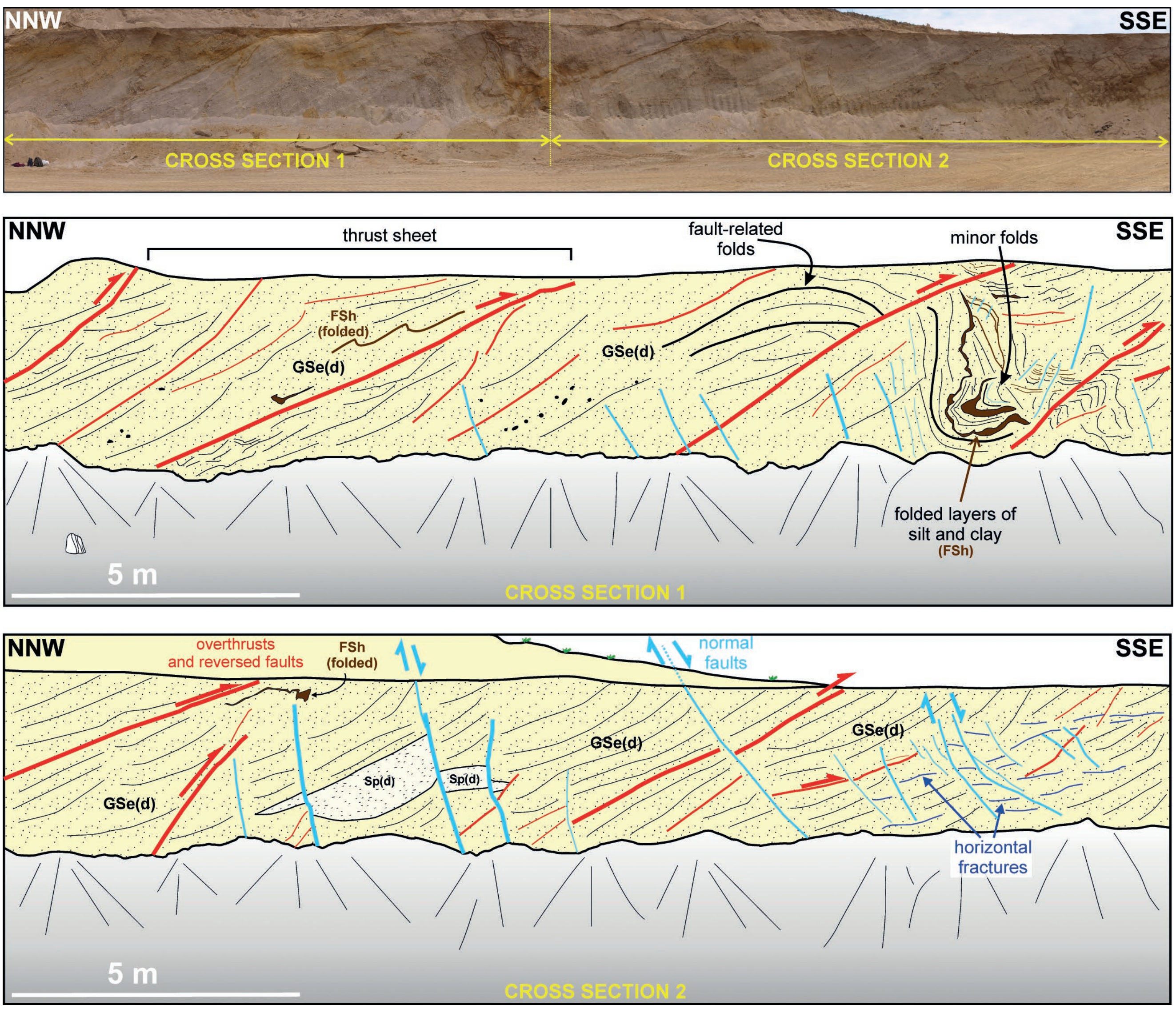

Fig. 8. Outcrop section at locality 2 in the central part of Czaple II Gravel Pit, with corresponding interpretive sketches, showing spatial distribution and relationships of the main glaciotectonic structures described in this paper (for further details, see text).

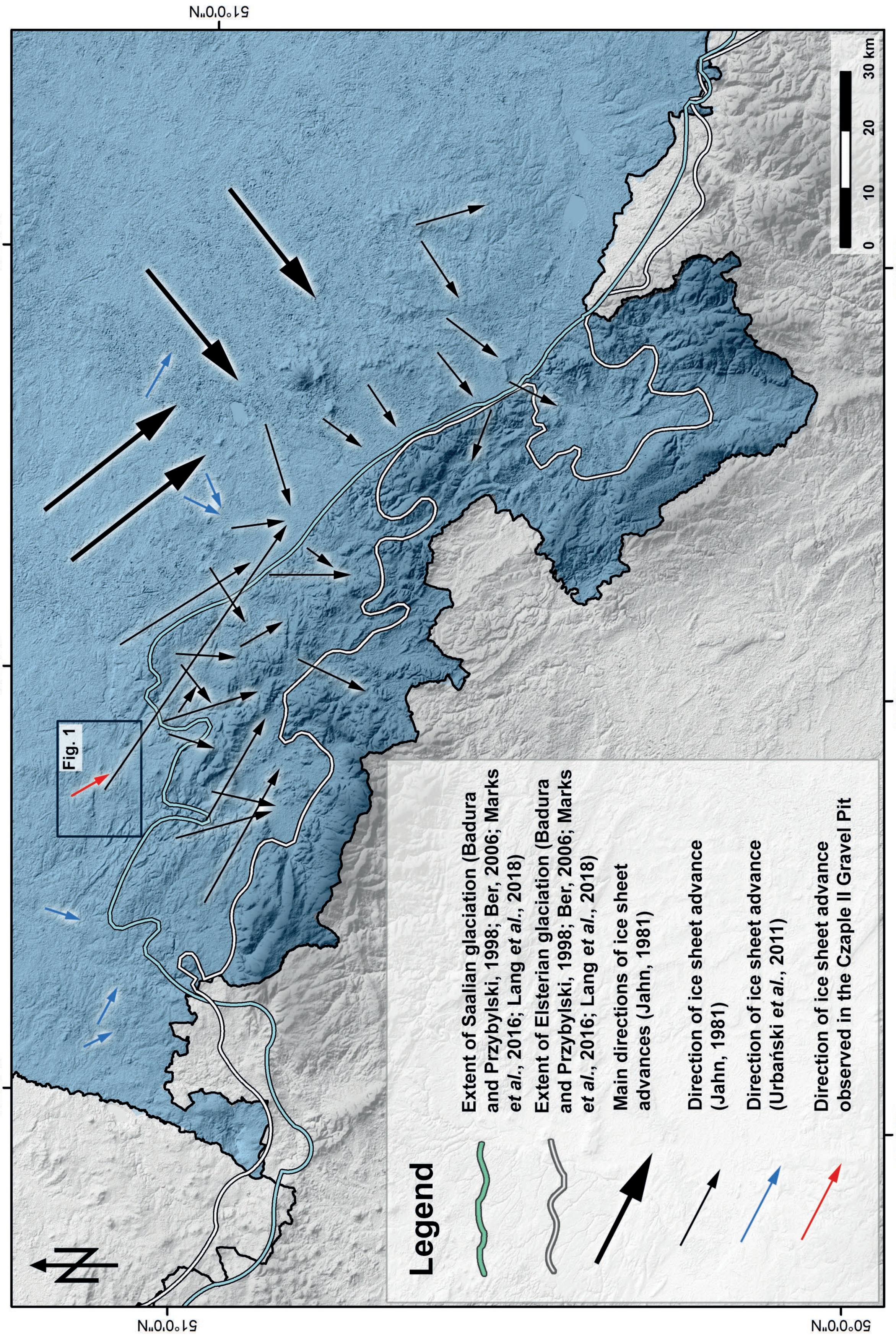

Fig. 9. Extent and advance direction of the Scandinavian Ice Sheet in Lower Silesia postulated by various authors for the Saalian and Elsterian glaciations (based on Ber, 2006). Digital terrane- elevation model from Aster GDEM (v2) software.

acting as lubricant layers for shearing (cf. Phillips, 2018). Kinematic analysis in the present case indicates thrusting direction towards the SSE and SE. The basal detachment (floor thrust) of the thrust-sheet deformation wedge is unexposed within the depth limit of the pit outcrop, and hence it is uncertain if the deformation reached the local bedrock at a depth of up to 30–40 m (cf. Milewicz and Jerzmański, 1959; Milewicz, 1961). This possibility is likely, as the depth extent of gleciotectonic deformation in the southern part of Lower Silesia has been regionally estimated at ca. 50 m (Ber *et al.*, 2004).

The subglacial till unit above the thrust-sheet pile indicates that the ice margin had overridden its push-formed thrust wedge after a modest initial bulldozing effect (cf. Aber *et al*, 1989). This implies a modest magnitude of thrust-wedge shortening and upward growth. The glacier overriding the thrust-sheet wedge was probably sliding over it, with the main strain dissipated within the basal till and the deeper deformation declining downwards (cf. Boulton and Hindmarsh, 1987; Benn, 1995; Boulton, 1996). At least some of the secondary features within the thrust-sheet wedge can be attributed to this stage of secondary deformation. For example, the secondary folds associated with faults (fault-propagation folds; cf. Brandes and Le Heron, 2010) in the thrust sheets occur above the fault surfaces in their hanging walls and are developed as a compensation of excess fault slip in conditions of an increased normal stress (Brandes and Le Heron, 2010). The SSE vergence of these secondary folds is consistent with the kinematics of the fault planes and the SE direction of ice-sheet movement (Fig. 4E, F). Similarly, the S- and SSW-dipping normal dip-slip faults that cut across the thrust sheets and displace their bounding fault planes (Figs 5A, B, 8) may be related to the normal stress of the advancing ice mass (cf. Aber, 1982). This interpretation is supported by the evidence of low-angle contractional joints and nearly horizontal small faults (Fig. 5C, D) that formed due to vertical compression. This implies that the associated normal faults, antithetic faults and horizontal fractures form conjugate sets (Fig. 5D, F) developed under the same stress conditions (e.g. Peacock *et al*., 2016). Secondary glaciotectonic structures include also the SSE-dipping dip-slip faults with small throw (Fig. 5E) that formed in the frontal parts of thrusts sheets and are consistent with the SE direction of ice movement (cf. Włodarski, 2009).

The complex pattern of deformation in the till unit and the underlying fine-grained glaciolacustrine deposits is typical of a subglacial shear zone (van den Wateren *et al.*, 2000; Phillips *et al*., 2008), where deformation occurs as simple shear under the load of an advancing glacier. The sets of SE-verging recumbent folds, parasitic folds and sheet folds (Fig. 6A, B) are consistent with a SE-directed progressive compression including normal-stress component. This interpretation is supported by the pattern of shear planes and the fabric of rotated and sheared gravel clasts in the till unit (Fig. 7).

Regional implications

It has long been recognized that the Scandinavian Ice Sheet reached Sudetes at least twice (Woldstedt, 1932; Lindner 1939; Dumanowski, 1950; Szczepankiewicz, 1952; Walczak, 1954; Jahn, 1960), but its exact areal extent and number of advances at this southern extremity remain poorly known and controversial. For example, Michniewicz *et al*. (1996) postulated one single ice-sheet advance reaching Sudetes, labelled as the South-Polish Glaciation (Elsterian, MIS 12), whereas Badura and Przybylski (1998) had recognized as many as three separate glacial-till levels in the Lower Silesia. The whole issue is further complicated by the fact that a reliable dating of the Pleistocene terrestrial glacial deposits is practically impossible. The present study follows the prevalent view that the deposits in the study area represent the Odranian Stadial (Saalian I, MIS 6) of the Mid-Polish Glaciations (Przybylski et al., 2009). The lowermost glacial-till unit, known from boreholes and unexposed in the gravel pit, is thought to be a relic of the South Polish Glaciation (Elsterian, MIS 12).

It may then seem puzzling that the deformed fluvioglacial deposits in the outcrop section show mainly northward palaeoflow directions, opposite to those expected for an proglacial outwash plain (cf. Edwards, 1978) suggested by previous authors (Milewicz and Jerzmański, 1959; Przybylski *et al*., 2009). However, it should be kept in mind that the Scandinavian Ice Sheet at its Sudetic extremity was effectively climbing onto a mountainous terrane that certainly hosted a large snowpack and possibly some Alpine-type small ice caps, and that their meltwater release would likely dominate the terrane during the climate amelioration and ice-sheet retreat. The fluvial sedimentation in the study area occurred during an interglacial episode of 'deglaciation' (cf. Szponar, 1986), between the Sanian II Glaciation represented by the lower (unexposed) till unit and the Saalian I Glaciation represented by the upper till unit. The interglacial sedimentation in the Sudetic foothill highland would then likely be dominated by N-directed fluvial drainage that virtually reworked the glacier's own outwash, leaving only its minor relics. This interpretive notion is supported by the compositional 'dilution' of exotic northerly rock debris in fluvial deposits (Fig. 2) and the palaeocurrent data from these deposits (see earlier text). The topographically controlled interglacial amalgamation of mountain-derived and glacier-derived outwash, amplified by the subsequent Odranian glaciotectonic deformation, may explain further the relatively great thickness of Pleistocene deposits in the study area – the main reason for their local mining.

CONCLUSIONS

The present study documents large-scale glaciotectonic deformation of Pleistocene deposits exposed in the Czaple II Gravel Pit of Lower Silesia, SW Poland, and thereby contributes to the existing sparse knowledge on the regional extent and dynamics of the Scandinavian Ice-Sheet front at its southernmost reaches in the mountainous region of Sudetes.

The Pleistocene sedimentary succession in the study area consists of glaciotectonically deformed fluvial outwash and lacustrine deposits sandwiched between two separate units of subglacial till. The study postulates that the fluvial to lacustrine sedimentation occurred at the interglacial stage between the Sanian II and Saalian I (Odranian) ice-sheet regional advances.

The study demonstrates that the meltwater drainage from the snowpack and possible small icecaps of the Sudetes prevailed over the meltwater drainage from the retreating ice sheet, resulting in a paradoxical outwash succession dominated by fluvial transport directed towards the ice-sheet front.

The study documents an interesting interplay of proglacial sedimentation and proglacial to subglacial deformation, where the lithology of interglacial sediments and the regional bedrock topography played an important role. The Odranian ice-sheet advance in the study area involved an initial phase of substrate deformation by simple push-type bulldozing, followed quickly – due to a lubricant argillaceous substrate – by an overriding by the glacier and a load-and-shear style of subglacial deformation. The structural heterogeneity of the Odranian till unit suggests further that its glaciotectonic deformation may have been multiple, recording shorter-term oscillations of the ice-sheet front.

Acknowledgements

The use of LiDAR data in the present study was granted by the academic license no. DIO.DFT.DSI.7211.1619.2015_PL_N issued to the University of Wrocław by the Polish national Head Office of Geodesy and Cartography. The authors thank Bogusław Przybylski and Dariusz Ciszek (PGI-NRI Wrocław) for constructive comments and numerous discussions during the preparation of this paper. Anna Żylińska kindly verified linguistically the initial version of the manuscript. Constructive and inspiring comments from Jonathan Lee (British Geological Survey) and an anonymous reviewer helped to improve the manuscript, which was further edited by Wojciech Nemec on behalf of the journal editors.

REFERENCES

Aber, J. S., 1982. Model for glaciotectonism. *Bulletin of the Geological Society of Denmark*, 30: 79–90.

Aber, J. S. & Ber, A., 2007. *Glaciotectonism. Development in Quaternary Science,* 6. Elsevier, Amsterdam, 246 pp.

Aber, J. S., Croot, D. G. & Fenton, M. M., 1989. *Glaciotectonic Landforms and Structures*. Kluwer, Dordrecht. 206 pp.

Alsop, G. I. & Holdsworth, R. E., 2006. Sheath folds as discriminators of bulk strain type. *Journal of Structural Geology*, 28: 1588–1606.

Awdankiewicz, M., 2006. Fractional crystallization, mafic replenishment and assimilation in crustal magma chambers: geochemical constraints from the Permian post-collisional intermediate-composition volcanic suite of the North-Sudetic Basin (SW Poland). *Geologia Sudetica*, 38: 39–61.

Badura, J., 2005. *Szczegółowa mapa geologiczna Polski, 1:50 000, arkusz Bolesławiec (721)*. Wydawnictwa Geologiczne, Warszawa. [In Polish.]

Badura, J. & Przybylski, B., 1998. Extent of the Pleistocene ice sheets and deglaciation between the Sudeten and the Silesian rampart. *Biuletyn Państwowego Instytutu Geologicznego*, 385: 9–28. [In Polish, with English abstract.]

Badura, J. & Przybylski, B., 2002. Multiphase development of glaciotectonic disturbances in the Lower Silesia. *Uniwersytet Zielonogórski*, *Zeszyty Naukowe,* 129*, Inżynieria Lądowa i Środowiskowa*, 37: 15–26. [In Polish, with English abstract.]

Badura, J., Zuchiewicz, W., Štěpančíková, P., Przybylski, B., Kontny, B. & Cacoń, S., 2007. The Sudetic Marginal Fault: a young morphophotectonic feature at the NE margin of the Bohemian Massif, Central Europe. *Acta Geodynamica et Geomaterialia*, 4: 7–29.

Banham, P. H., 1975. Glaciotectonic structures: a general discussion with particular reference to the contorted drift of Norfolk. In: Wright, A. E. & Moseley, F. (eds), *Ice Ages: Ancient and Modern*. Seel House Press, Liverpool, pp. 69–84.

Banham, P. H., 1977. Glaciotectonites in till stratigraphy. *Boreas,* 6: 101–105.

Banham, P. H., 1988. Polyphase glaciotectonic deformation in the contorted drift of Norfolk. In: Croot, D. (Ed.), *Glacio-tectonics: Forms and Processes*. Balkema, Rotterdam, pp. 7–32.

Baranowski, Z., Haydukiewicz, A., Kryza, R., Lorenc, S., Muszyński, A., Solecki, A. & Urbanek Z., 1990. Outline of the geology of the Góry Kaczawskie (Sudetes, Poland). *Neues Jahrbuch für Geologie und Paläontologie*, 179: 223–257.

Benediktsson, Í. Ö., Møller, P., Ingólfsson, Ó., van der Meer, J. J. M., Kjær, K. H. & Kröger, J., 2008. Instantaneous end moraine and sediment wedge formation during the 1890 glacier surge of Brúarjökull, Iceland. *Quaternary Science Reviews*, 27: 209–234.

Benn, D. I., 1995. Fabric signatur e of subglacial till deformation, Breidamerkurjrkull, Iceland. *Sedimentology*, 42: 735–747.

Ber, A., 2006. *Glaciotectonic Map of Poland, 1:1 000 000*. Państwowy Instytut Geologiczny, Warszawa. [In Polish, with English summary.]

Ber, A., Dobracki, R., Lisicki, S., Morawski, W., Badura, J., Krzyszkowski, D., Przybylski, B., Urbański, K., Kasprzak, L., Ruszczyńska-Szenajch, H., Wysota, W., Turkowska, K., Gardziel, Z., Harasimiuk, M., Lewandowski, J. & Wójcik, A., 2004. Glaciotectonics of the selected regions of Poland. *Biuletyn Państwowego Instytutu Geologicznego*, 408: 73–125. [In Polish, with English summary.]

Beyer, K., 1933. Die nordsudetische Rahmenfaltung. *Abhandlungen der Naturforschenden Gesellschaft zu Görlitz*, 32: 121–172.

Boulton, G. S., 1996. Theory of glacial erosion, transport and deposition as a consequence of subglacial sediment deformation. *Journal of Glaciology*, 42: 43–62.

Boulton, G. S. & Hindmarsh, R. C. A., 1987. Sediment deformation beneath glaciers: rheology and geological consequences. *Journal of Geophysical Research, Solid Earth*, B92: 9059–9082.

Brandes, C. & Le Heron, D. P., 2010. The glaciotectonic deformation of Quaternary sediments by fault-propagation folding. *Proceedings of the Geologists' Association*, 121: 270–280.

Brodzikowski, K. & Van Loon, A. J., 1987. A systematic classification of glacial and periglacial environments, facies and deposits. *Earth-Science Reviews*, 24: 297–381.

Christiansen, E. A. & Whitaker, S. H., 1976. Glacial thrusting of drift and bedrock. In: Leggett, R. F. (ed.), *Glacial Till. Royal Society of Canada, Special Publication,* 12: 121–130.

Chrząstek, A., 2002. Stratigraphy and sedimentation condition of Röt and Lower Muschelkalk of the North Sudetic Basin. *Acta Universitatis Wratislaviensis,* 2383*, Prace Geologiczno-Mineralogiczne*, 73: 1–128. [In Polish, with English summary.]

Chrząstek, A. & Wojewoda, J., 2011. Mesozoic of South-Western Poland (the North Sudetic Synclinorium). In: Żelaźniewicz, A., Wojewoda, J. & Ciężkowski, W. (eds) *Mezozoik i kenozik Dolnego Śląska*. WIND, Wrocław, pp. 1–10. [In Polish, with English abstract.]

Croot, D. G., 1987. Glacio-tectonic structures: a mesoscale model of thin-skinned thrust sheets? *Journal of Structural Geology*, 9: 797–808.

Cymerman, Z., 2002. Structural and kinematic analysis and the Variscan tectonic evolution of the Kaczawa Complex (the Sudetes). *Prace Państwowego Instytutu Geologicznego*, 65: 1–143. [In Polish, with English summary.]

Cymerman, Z., 2004. *Tectonic Map of the Sudetes and the Fore-Sudetic Block, 1:200 000*. Państwowy Instytut Geologiczny, Warszawa.

Cymerman, Z., Ihnatowicz, A., Kozdrój, W. & Przybylski, B., 2005. *Szczegółowa mapa geologiczna Polski, 1:50 000, arkusz Lwówek Śląski (758)*. Wydawnictwa Geologiczne, Warszawa. [In Polish.]

Dove, D., Evans, D. J. A., Lee, J. R., Roberts, D. H., Tappin, D. R., Mellett, C. L., Long, D. & Callard, S. L., 2017. Phased occupation and retreat of the last British–Irish Ice Sheet in the southern North Sea: geomorphic and seismostratigraphic evidence of a dynamic ice lobe. *Quaternary Science Reviews*, 163: 114–134.

Dumanowski, B., 1950. Morfologia doliny Bobru w okolicy Jeleniej Góry. *Czasopismo Geograficzne*, 21/22: 403–411. [In Polish.]

Dumanowski, B., 1961. The problem of bipartition of tills in the Sudeten Mts. *Annales Societatis Geologorum Poloniae*, 31: 319–333. [In Polish, with English summary.]

Edwards, M. B., 1978. Glacial environments. In: Reading, H. G. (ed.), *Sedimentary Environments and Facies*. Blackwell, Oxford, pp. 416–438.

Ehlers, J., 1990. Reconstructing the dynamics of the north-west European Pleistocene ice sheets. *Quaternary Science Reviews*, 9: 71–83.

Evans, D. J. A., 2007. Glacitectonic structures and landforms. In: Elias, S. A. (ed.), *Encyclopedia of Quaternary Science*. Elsevier, Oxford, pp. 831–838.

Eyles, N., Eyles, C. H. & Miall, A. D., 1983. Lithofacies types and vertical profile models: an alternative approach to the description and environmental interpretation of glacial diamict and diamictite sequences. *Sedimentology*, 30: 393–410.

Fossen, H., 2010. *Structural Geology*. Cambridge University Press, New York, 463 pp.

Fossen, H., Schultz, R. A., Shipton, Z. K. & Mair, K., 2007. Deformation bands in sandstone: a review. *Journal of the Geological Society*, 164: 755–769.

Girard, F., Ghienne, J. F., Du-Bernard, X. & Rubino, J. J., 2015. Sedimentary imprints of former ice-sheet margins: Insights from an end-Ordovician archive (SW Libya). *Earth-Science Reviews*, 148: 259–289.

Górecka, T., 1970. Results of microfloristic research of Permo-Carboniferous deposits found in the area between Jawor and Lubań. *Kwartalnik Geologiczny*, 14: 52–64. [In Polish, with English summary.]

Gradziński, M., Hercman, H. & Staniszewski, K., 2014. Middle Pleistocene carbonate-cemented colluvium in southern Poland: Its depositional processes, diagenesis and regional palaeoenvironmental significance. *Sedimentary Geology*, 306: 24–35.

Hartshorn, J. H., 1958. Flowtill in southeastern Massachusetts. *Geological Society of America Bulletin*, 69: 477–482.

Jahn, A., 1960. Czwartorzęd Sudetów. In: Teisseyre, H. (ed.), *Regionalna geologia Polski, tom III, Sudety*. Polskie Towarzystwo Geologiczne, Kraków, pp. 357–418. [In Polish.]

Jahn, A., 1976. „Diurnal” varved clays from Jelenia Góra. *Przegląd Geologiczny*, 24: 517–520. [In Polish, with English summary.]

Jahn, A., 1981. Notes on the movement of the Pleistocene ice sheet in Lower Silesia. *Biuletyn Państwowego Instytutu Geologicznego*, 321: 117–130. [In Polish with English summary.]

Jarecki, S., 2009. *Dokumentacja geologiczna w kategorii C1 złoża kruszywa naturalnego Czaple II, miejscowość Czaple, gmina Pielgrzymka, powiat złotoryjski, województwo dolnośląskie*. Unpublished report. Centralne Archiwum Geologiczne, Państwowy Instytut Geologiczny – Państwowy Instytut Badawczy, Warszawa, 55 pp. [In Polish.]

Jaroszewski, W., 1991. Considerations on the origin of glaciotectonic structures. *Annales Societatis Geologorum Poloniae*, 61: 153–206. [In Polish, with English summary.]

Johnstrup, F., 1874. Ueber die Lagerungsverhaltnisse und die Hebungs-phiinomene in den Kreidefelsen auf Moen und Rugen. *Zeitschrift der Deutschen Gesellschaft für Geowissenschaften,* 1874: 533–585.

Kondracki, J., 2002. *Geografia regionalna Polski*. PWN, Warszawa, 441 pp. [In Polish.]

Kozdrój, W., Ihnatowicz, A. & Przybylski, B., 2005. *Szczegółowa mapa geologiczna Polski, 1:50 000, arkusz Złotoryja (759)*. Wydawnictwa Geologiczne, Warszawa. [In Polish.]

Kozłowski, S. & Parachoniak, W., 1967. Wulkanizm permski w depresji północnosudeckiej, *Prace Muzeum Ziemi*, 11: 191–221. [In Polish.]

Krygowski, B., 1952. The Quaternary of the Grodziska Basin. *Biuletyn Instytutu Geologicznego, 65:* 417–466. [In Polish, with English summary.]

Krysiak, Z., 2007. Mesostructural analysis of glaciotectonic structures and its application to reconstruction of the ice sheet advance directions. *Biuletyn Państwowego Instytutu Geologicznego*, 425: 35–46. [In Polish, with English summary.]

Kryza, R. & Muszyński, A., 1992. Pre-Variscan volcanic-sedimentary succession of the central southern Góry Kaczawskie, SW Poland: outline geology. *Annales Societatis Geologorum Poloniae*, 62: 117–140.

Krzyszkowski, D., 1996. Glaciotectonic deformation during the Elsterian ice-sheet advance at the northeastern margin of the Sudetic Foreland, SW Poland. *Boreas*, 25: 209–226.

Krzyszkowski, D. & Czech, A., 1995. Directions of the Pleistocoene ice-sheet advances in the northern margin of the Strzegom Hills, Sudetic Foreland (SW Poland). *Przegląd Geologiczny,* 43: 647–651. [In Polish, with English abstract.]

Krzyszkowski, D. & Stachura, R., 1998. Late Quaternary valley formation and neotectonic evolution on the Wałbrzych Upland, Middle Sudeten Mts., southwestern Poland. *Annales Societatis Geologorum Poloniae*, 68: 23–60.

Lang, J., Lauer, T. & Winsemann, J., 2018. New age constraints for the Saalian glaciation in northern central Europe: Implications for the extent of ice sheets and related proglacial lake systems. *Quaternary Science Reviews*, 180*:* 240–259.

Lee, J. R. & Phillips, E., 2013. Glacitectonics – a key approach to examining ice dynamics, substrate rheology and ice-bed coupling. *Proceedings of the Geologists' Association*, 124: 731–737.

Lee, J. R., Phillips, E., Booth, S. J., Rose, J., Jordan, H. M., Pawley, S. M., Warren M. & Lawley, R. S., 2013. A polyphase glacitectonic model for ice-marginal retreat and terminal moraine development: the Middle Pleistocene British Ice Sheet, northern Norfolk, UK. *Proceedings of the Geologists' Association*, 124: 753–777.

Lee, J. R., Phillips, E., Rose, J. & Vaughan Hirsch, D., 2017. The Middle Pleistocene glacial evolution of northern East Anglia, UK: a dynamic tectonostratigraphic–parasequence approach. *Journal of Quaternary Science*, 32: 231–260.

Leszczyński, S., 2018. Integrated sedimentological and ichnological study of the Coniacian sedimentation in North Sudetic Basin, SW Poland. *Geological Quarterly,* 62: 767–816.

Lindner, H., 1939. Die Gnadenfelder saaleeiszeitliche Endstaffel und die Bewegungen des Saale-Eises in Oberschlesien. *Jahresberichte der Geologischen Vereinigung Oberschlesiens*, 1939, II: 1–19.

Lindner, L. & Marks, L., 2012. Climatostratigraphic subdivision of the Pleistocene Middle Polish complex in Poland. *Przegląd Geologiczny*, 60: 36–45. [In Polish, with English abstract.]

Lyell, C., 1863. *The Geological Evidences of the Antiquity of Man.* 3rd ed., John Murray, London, 300 pp.

Marks, L., Karabanov, A., Nitychoruk, J., Bahdasarau, M., Krzywicki, T., Majecka, A., Pochocka-Szwarc, K., Rychel, J., Woronko, B., Zbucki, Ł., Hradunova, A., Hrychanik, M., Mamchyk, S., Rylova, T., Nowacki, Ł. & Pielach, M., 2016. Revised limit of the Saalian ice sheet in central Europe. *Quaternary International*, 478: 59–74.

Mastalerz, K. & Wojewoda, J., 1990. The pre-Kaczawa alluvial fan – an example of sedimentation in an active wrench zone, Plio-Pleistocene age, Sudetic Mountains. *Przegląd Geologiczny*, 38: 363–370. [In Polish, with English summary.]

McCarroll, D. & Rijsdijk, K. F., 2003. Deformation styles as a key for interpreting glacial depositional environments. *Journal of Quaternary Science*, 18: 473–489.

Miall, A. D., 1985. Architectural element analysis: a new method of facies analysis applied to fluvial deposits. *Earth-Science Reviews,* 22: 261–308.

Michniewicz, M., Czerski, M., Kiełczawa, J. & Wojtkowiak, A., 1996. Early Pleistocene buried valleys system of Western Sudetes and its foreland (SW Poland). *Przegląd Geologiczny,* 44: 1232–1238. [In Polish, with English summary.]

Migoń, P. & Łach, J., 1998. Geomorphological evidence of neotectonics in the Kaczawa sector of the Sudetic Marginal Fault, southwestern Poland. *Geologia Sudetica*, 31: 307–316.

Mierzejewski, M., 1959. Contribution to the knowledge of glaci-tectonic phenomena in Lower Silesia. *Biuletyn Instytutu Geologicznego*, 146: 119–127. [In Polish with English summary.]

Milewicz, J., 1961. *Szczegółowa mapa geologiczna Sudetów, 1:25 000, arkusz Skorzynice (20).* Wydawnictwa Geologiczne, Warszawa. [In Polish.]

Milewicz, J., 1985. A proposal of formal stratigraphic subdivision of the infill of the North Sudetic Depression. *Przegląd Geologiczny*, 33: 385–389. [In Polish, with English summary.]

Milewicz, J., 1997. Upper Cretaceous of the North Sudetic depression (litho- and biostratigraphy, tectonics and remarks on raw materials). *Acta Universitatis Wratislaviensis*, 1971*, Prace Geologiczno-Mineralogiczne*, 61*:* 1–58. [In Polish, with English summary.]

Milewicz, J. & Górecka, T., 1965. Preliminary remarks on the Carboniferous in the North-Sudetic Depression. *Kwartalnik Geologiczny*, 9: 113–114. [In Polish, with English summary.]

Milewicz, J. & Jerzmański, J., 1959. *Szczegółowa mapa geologiczna Sudetów, 1:25 000, arkusz Pielgrzymka (21)*. Wydawnictwa Geologiczne, Warszawa. [In Polish.]

Mroczkowski, J., 1972. Sedimentation of the Bunter in the Northsudetic Basin. *Acta Geologica Polonica*, 22: 35–377. [In Polish, with English summary.]

Peacock, D. C. P., Nixon, C. W., Rotevatn, A., Sanderson, D. J. & Zuluaga, L. F., 2016. Glossary of fault and other fracture networks. *Journal of Structural Geology*, 92: 12–29.

Pedersen, S. A. S., 1987. Comparative studies of gravity tectonics in Quaternary sediments and sedimentary rocks related to fold belts. In: Jones, M. E. & Preston, R. M. F. (eds), *Sediment Deformation Mechanisms. Geological Society of London, Special Publication,* 29: 43–65.

Pedersen, S. A. S., 2000. Superimposed deformation in glaciotectonics. *Bulletin of the Geological Society of Denmark*, 46: 125–144.

Pedersen, S. A. S., 2005. Structural analysis of the Rubjerg Knude Glaciotectonic Complex, Vendsyssel, northern Denmark. *Geological Survey of Denmark and Greenland Bulletin*, 8: 1–192.

Pedersen, S. A. S., 2014. Architecture of glaciotectonic complexes. *Geosciences,* 4: 269–296.

Petit, J. P., 1987. Criteria for the sense of movement on fault surfaces in brittle rocks. *Journal of Structural Geology*, 9: 597–608.

Phillips, E. R., 2018. Glacitectonics. In: Menzies, J. & van der Meer J. J. M. (eds), *Past Glacial Environments.* 2nd ed., Elsevier, London, pp. 467–502.

Phillips, E., Evans, D. J. A., Atkinson, N. & Kendall, A., 2017. Structural architecture and glacitectonic evolution of the Mud Buttes cupola hill complex, southern Alberta, Canada. *Quaternary Science Reviews*, 164: 110–139.

Phillips, E. & Lee, J. R., 2011. Description, measurement and analysis of glacitectonically deformed sequences. In: Phillips, E., Lee, J. R. & Evans, H. M. (eds), *Glacitectonics – Field Guide.* Quaternary Research Association, pp. 5–31.

Phillips, E., Lee, J. R. & Burke, H., 2008. Progressive proglacial to subglacial deformation and syntectonic sedimentation at the margins of the Mid-Pleistocene British Ice Sheet: evidence from north Norfolk, UK. *Quaternary Science Reviews*, 27: 1848–1871.

Pitura, M., Sobczyk, A. & Dąbrowski, M., 2017. Glacial isostasy numerical modelling in the Sudetes Mts. after Elsterian glaciation. In: Twardy, J. (ed.), *Czwartorzęd pogranicza niżu i wyżyn w Polsce Środkowej. XXIV Konferencja Naukowo-Szkoleniowa Stratygrafia Plejstocenu Polski*, Uniwersytet Łódzki, Łódź, pp. 117–118. [In Polish.]

Przybylski, B., Cymerman, Z., Ihnatowicz, A. & Kozdrój, W., 2009. *Objaśnienia do szczegółowej mapy geologicznej Polski, 1:50 000, arkusz Lwówek Śląski (758).* Państwowy Instytut Geologiczny, Warszawa, 55 pp. [In Polish.]

Raczyński, P., 1997. Depositional conditions and paleoenvironments of the Zechstein deposits in the North-Sudetic Basin (SW Poland). *Przegląd Geologiczny*, 45: 693–699. [In Polish, with English summary.]

Raumer, K. von, 1819. *Das Gebirge Nieder-Schlesiens, der Grafschaft Glatz und eines Theils von Böhmen und der Ober-Lausitz geognostisch dergestelt*. Walter De Gruyter, Berlin. 184 pp.

Rocha-Campos, A. C., Canuto, J. R. & Dos Santos, P. R., 2000. Late Paleozoic glaciotectonic structures in northern Paraná Basin, Brazil. *Sedimentary Geology*, 130: 131–143.

Roman, M., (in press). Ice-flow directions of the last Scandinavian Ice Sheet in central Poland. *Quaternary International,* doi.org/10.1016/j.quaint.2017.11.035.

Rotnicki, K., 1976. The theoretical basis for and a model of the origin of glaciotectonic deformations. *Quaestiones Geographicae*, 3: 103–139.

Ruszczyńska-Szenajch, H., 1985. Origin and age of the large-scale glaciotectonic structures in central and eastern Poland. *Annales Societatis Geologorum Poloniae,* 55: 307–332.

Scupin, H., 1913. *Die Löwenberger Kreide und ihre Fauna*. Palaeontographica Palaeontographica Supplement 6, E. Schweizerbart, Stuttgart, 275 pp.

Scupin, H., 1933. Der Buntsandstain der Nordsudeten. *Zeitschrift der Deutschen Geologischen Gesellschaft*, 85: 161–189.

Shilts, W. W., 1976. Glacial till and mineral exploration. In: Legget, R. F. (ed.), *Glacial Till. Royal Society of Canada, Special Publication*, 12: 205–224.

Slater, G., 1926. Glacial tectonics as reflected in disturbed drift deposits. *Geologists' Association Proceedings*, 37: 392–400.

Solecki, A., 2011. Structural development of the epi-Variscan cover in the North Sudetic Synclinorium area. In: Żelaźniewicz, A., Wojewoda, J. & Ciężkowski, W. (eds) *Mezozoik i kenozik Dolnego Śląska*. WIND, Wrocław, pp. 19–36. [In Polish, with English abstract.]

Szczepankiewicz, S., 1952. The Development of the Valley of Upper Bóbr (Bober) in the Sudetes at the Edge of the Ice Sheet. *Czasopismo Geograficzne,* 23/24: 122–137. [In Polish, with English summary.]

Szponar, A., 1986. Chronostratigraphy and the stages of deglaciations in the Sudetes foreland area in the period of the Middle-Polish Glaciation. *Acta Universitatis Wratislaviensis*, 963, *Studia Geograficzne,* 45: 1–202. [In Polish, with English summary.]

Sztromwasser, E., 1995. *Szczegółowa mapa geologiczna Polski, 1:50 000, arkusz Chojnów (722)*. Wydawnictwa Geologiczne, Warszawa. [In Polish.]

Śliwiński, W., Raczyński, P. & Wojewoda, J., 2003. Sedymentacja utworów epiwaryscyjskiej pokrywy osadowej w basenie północnosudeckim. In: Ciężkowski, W., Wojewoda, J. & Żelaźniewicz, A. (eds), *Sudety Zachodnie: od wendu do czwartorzędu*. WIND, Wrocław, pp. 119–126. [In Polish.]

Teisseyre, H., Smulikowski, K. & Oberc, J., 1957. *Regionalna geologia Polski. tom III, Sudety; zeszyt 1, Utwory przedtrzeciorzędowe*. Polskie Towarzystwo Geologiczne, Kraków, 300 pp. [In Polish.]

Urbański, K., 2002. Glacitectonic deformation of Ziemia Lubuska. *Uniwersytet Zielonogórski, Zeszyty Naukowe*, 129, *Inżynieria Lądowa i Środowiskowa*, 37: 159–173. [In Polish, with English abstract.]

Urbański, K., 2007. The zones of glaciotectonical deformation in Muskau Arc region. *Uniwersytet Zielonogórski, Zeszyty Naukowe*, 134, *Inżynieria Środowiska*, 14: 179–190. [In Polish, with English summary.]

Urbański, K., 2009. Glaciotectonic deformations in the Sudetic Foreland within tectonic block structures of the Wądroże Wielkie area. *Prace Państwowego Instytutu Geologicznego*, 194: 63–74. [In Polish, with English summary.]

Urbański, K., Hałuszczak, A. & Różański, P., 2011. Glacitectonic deformation in southern part of Silesian Lowland and Sudetic Forland. In: Żelaźniewicz, A., Wojewoda, J. & Ciężkowski, W. (eds) *Mezozoik i kenozik Dolnego Śląska*. WIND, Wrocław, pp. 9–78. [In Polish, with English abstract.]

Van der Wateren, F. M., 1985. A model of glacial tectonics, applied to the ice-pushed ridges in the central Netherlands. *Bulletin of the Geological Society of Denmark*, 34: 55–77.

Van der Wateren, F. M., 1995. Structural geology and sedimentology of push moraines. *Mededelingen Rijks Geologische Dienst,* 54: 1–168.

Van der Wateren, F. M., Kluiving, S. J. & Bartek, L. R., 2000. Kinematic indicators of subglacial shearing. In: Maltman, A., Hubbard, B. & Hambrey, M. J. (eds), *Deformation of Glacial Materials. Geological Society of London, Special Publication*, 176: 259–278.

Wachecka-Kotkowska, L., 2015. Measurements of till fabric orientation in the morainic tills for reconstruction of the ice flow direction in the Piotrków Trybynalski, Radomsko and Przedbórz (Central Poland). *Acta Geographica Lodziensia*, 103: 99–115. [In Polish, with English summary.]

Walczak, W., 1954. The outwash valley of the Nysa River and the Pleistocene hydrographic changes in the foreland of the Eastern Sudetes. *Prace Geograficzne,* 2: 1–51. [In Polish, with English summary.]

Widera, M., 2018. Tectonic and glaciotectonic deformations in the areas of Polish lignite deposits. *Civil and Environmental Engineering Reports*, 28: 182–193.

Włodarski, W., 2009. Structural and kinematic analysis of glaciotectonic deformation complex within Kleczew graben zone (Konin elevation, Central Polish Lowland). *Prace Państwowego Instytutu Geologicznego*, 194: 75–100. [In Polish, with English summary.]

Włodarski, W., 2014. Geometry and kinematics of glaciotectonic deformation superimposed on the Cenozoic fault-tectonic framework in the central Polish Lowlands. *Quaternary Science Reviews*, 94: 44–61.

Wojewoda, J. & Mastalerz, K., 1989. Climate evolution, allo- and autocyclicity of sedimentation: an example from the Permo-Carboniferous continental deposits of the Sudetes, SW Poland. *Przegląd Geologiczny*, 432: 173–180. [In Polish, with English summary.]

Woldstedt, P., 1932. Über Endmoränen und Oser der Saale (= Riss) Vereisung in Schlesien. *Zeitschrift für Deutschen Geologischen Gesselschaften*, 84: 78–84.

Wójcik, J., 1985. Directions of advance od mid-polish glaciation icesheet in the light of petrographic composition of moraines in area between the Jelenia Góra depression and Góry Sowie

Block, Sudety Mts. *Kwartalnik Geologiczny*, 29: 437–458. [In Polish, with English summary.]

Wójcik, J., 1996. Transgresja lądolodu zlodowacenia środkowopolskiego w Sudety. *Przegląd Geologiczny*, 44: 579–583. [In Polish.]

Wójcik, Z., 1960. Characteristic of glacitectonic foldings in Turoszów (Lower Silesia). *Przegląd Geologiczny*, 12: 633–637. [In Polish, with English summary.]

Zieliński, T. & Pisarska-Jamroży, M., 2012. Which features of deposits should be included in a code and which not? *Przegląd Geologiczny,* 60: 387–397. [In Polish, with English abstract.]

Zieliński, T. & Van Loon, A. J., 1999. Subaerial terminoglacial fans, II: a semi-quantitative sedimentological analysis of the middle and distal environments. *Geologie en Mijnbouw*, 78: 73–85.

Żelaźniewicz, A., Aleksandrowski, P., Buła, Z., Karnkowski P. H., Konon, A., Oszczypko, N., Ślączka, A., Żaba, J. & Żytko, K., 2011. *Regionalizacja tektoniczna Polski.* Komitet Nauk Geologicznych Polskiej Akademii Nauk, Wrocław, 60 pp. [In Polish.]